Korean J. Chem. Eng., 39(11), 3138-3145 (2022)
DOI: 10.1007/s11814-022-1168-2

pISSN: 0256-1115
eISSN: 1975-7220

Synthesis of polyethylenimine-modified magnetic hydrogel nanocomposite absorbents for heavy metals removal

Tao Wan*,,†, Songsong He**, Tairan Wang**, Jian Wang**, Mingrui Yu**, Yang Jia**, and Qi Tang****

*State Key Lab of Geohazard Prevention & Geoenvironment Protection, Chengdu University of Technology, Chengdu 610059, Sichuan, China
**Mineral Resources Chemistry Key Laboratory of Sichuan Higher Education Institutions, Chengdu University of Technology, Chengdu 610059, Sichuan, China
(*Received 25 March 2022 • Revised 3 May 2022 • Accepted 7 May 2022*)

Abstract−Polyethylenimine(PEI)-modified magnetic hydrogel nanocomposite absorbents (PEI-mHNAs) were fabricated based on poly(acrylamide-co-acrylic acid) and PEI-modified magnetic nanoparticles by radical copolymerization. FTIR and XRD results preliminarily confirmed the target structure of PEI-mHNAs without destroying the structure of magnetic nanoparticles during modification and radical copolymerization. PEI-mHNAs with many rough porous and interstitial structure had high adsorption capacity of Cu(II) (217 mg/g), Cd(II) (232 mg/g) and Pb(II) (459 mg/g). PEI-mHNAs had the best absorption capacity for heavy metal ions in the synthesis condition of acrylic acid/acrylamide mass ratio of 60 : 40, 0.8% initiator, AA neutralization degree of 70%, 0.75% crosslinker, and 15% PEI-modified magnetic nanoparticles. Moreover, PEI-mHNAs had good magnetic responsiveness, high thermal stability and reusability, which make it a potential application in removing heavy metal ions from the contaminated wastewater.

Keywords: Polyethylenimine, Hydrogel, Nanocomposite, Absorbent, Heavy Metals

INTRODUCTION

Environmental issues have always been a worldwide problem by the entire biosphere including plants and animals on earth, in which heavy metals pollution in water is one of the most challenges. As one of the most important substances for all living organisms, including plants and animals on the Earth, water covers almost 75% of the earth's surface, but less than 1% of it is available for human use [1]. However, the supply of fresh water is dwindling because of industrial activities such as mining, electroplating, and metal processing, releasing a large amount of wastewater contaminated by several toxic heavy metals [2]. Heavy metals such as copper, lead and cadmium are highly toxic even at very low concentration and can accumulate in living organisms, interrupting the food chain, causing severe disorders and diseases [3-5]. For example, copper can have adverse health impact such as haemolytic anaemia, neurological abnormalities, and even cancer [6]. Cadmium can cause renal dysfunction, bone degeneration, lung insufficiency, liver damage, and hypertension [7]. Lead can damage the central nervous system, brain, kidney, liver and reproductive system [8,9]. Therefore, the method of water purification for removing heavy metal ions such as copper, lead and cadmium has been highly concerned by the global scientific community.

Up to now, diverse methods have been reported for efficient heavy metals removal from wastewater. These include filtration, membrane separation, chemical precipitation, coagulation, sedimentation, reverse osmosis, electrodialysis, ion exchange, and adsorption [10-13]. Among these methods, adsorption has been shown to be a simple, low-cost, efficient, and eco-friendly methodology for decontaminating the heavy metal-containing wastewaters [14-20]. However, the regeneration of conventional adsorbents is complicated and there arises a necessity for further purification during the utilization of the adsorbents [21]. To overcome the disadvantages of the adsorbents, magnetic nanoadsorbents are employed in treating the heavy metal ions more specifically and effectively. In addition, magnetic nanoadsorbents facilitate separation of adsorbent from aqueous solution by using an external magnetic field [22,23]. Nevertheless, magnetic nanoadsorbents are easy to oxidize and agglomerate and have poor acid and alkali resistance. Hence, in order to avoid its aggregation and increase its stability against oxidation as well as acidic and alkaline media, the surface of magnetic nanoparticles was modified by polymer compounds with suitable functional groups such as natural polymers, e.g., chitosan and its derivatives [24], cellulose [25], poly(1-vinylimidazole) [26] as well as some copolymers, e.g., acrylic acid and crotonic acid [27-30]. However, disadvantages such as their low surface area and long contact time limited their use in practical wastewater treatment applications [21,31].

In recent years, hydrogel polymers with three-dimensional networks and functional groups have been widely used in the removal of heavy metals from aqueous solutions because of their abundant functional groups and porous structure [32-34]. As a typical water-soluble polyamine, polyethylenimine (PEI) contains a large number of nitrogen atoms of amine group. These amine groups have strong adsorption ability to heavy metals [35-37]. Therefore, PEI modified magnetic nanoparticles combine the magnetic proper-

†To whom correspondence should be addressed.
E-mail: wantaos@126.com

ties of MNPs and high heavy metals adsorption capacity of PEI [38]. If PEI modified magnetic nanoparticles can be combined with the hydrogel polymers, absorption capacity for heavy metals will be further improved. However, little has been reported on the preparation and its heavy metal absorption behavior of PEI-modified magnetic hydrogel nanocomposite absorbents based on poly(acrylamide-co-acrylic acid) and PEI-modified magnetic nanoparticles.

In this work, we fabricated PEI-modified magnetic hydrogel nanocomposite absorbents (PEI-mHNAs) with three-dimensional networks based on poly(acrylamide-co-acrylic acid) and PEI-modified magnetic nanoparticles. The effects of synthesis parameters such as acrylic acid/acrylamide mass ratio, initiator amount, AA neutralization degree, crosslinker amount and amount of PEI-modified magnetic nanoparticles on the adsorption capacities of heavy metal ions such as Cu(II), Cd(II) and Pb(II) were investigated. Structure, morphology and reusability of PEI-mHNAs were also evaluated.

MATERIALS AND METHODS

1. Materials

Acrylic acid (AA), acrylamide (AM), ammonium persulfate (APS), and sodium bisulfite (SBS) were purchased from Chengdu Kelong Reagent Chemicals (China). $FeCl_3 \cdot 6H_2O$, $FeCl_2 \cdot 7H_2O$ and γ-chloropropyl trimethoxy silane (CTS) were purchased from Chengdu Huaxia Reagent Chemicals (China). Polyethylenimine (PEI) and polyethylene glycol diacrylate (PEGD) were purchased from Chengdu Aike Chemical Reagent (China). All chemicals used were of analytical reagent grade without further purification.

2. Preparation of Magnetic Nanoparticles (MNPs)

Magnetic nanoparticles (MNPs) were synthesized according to a known procedure by co-precipitation method [39-41]. Typically, 19.6 g $FeCl_3 \cdot 6H_2O$) and 7.2 g $FeCl_2 \cdot 7H_2O$ were dissolved in deionized water (300 mL) and stirred at 60 °C. Then, 2 mol/L of ammonia solution was added dropwise under vigorous stirring until the pH reached 11 and the reaction mixture was stirred for 4.5 h. After cooling to room temperature, MNPs were separated by an external magnet and washed several times with deionized water. Finally, MNPs were dried at 60 °C for 24 h under vacuum.

3. Preparation of CTS-Modified Magnetic Nanoparticles (CTS-MNPs)

Typically, 1 g MNPs were dissolved in deionized water and ethanol (100 mL) and stirred at 50 °C under N_2 protection. Then, 1.5 mL 30% ammonia solution was added dropwise under vigorous stirring, followed by slow addition of 3 mL silane coupling agent (γ-chloropropyl trimethoxy silane, CTS) under vigorous stirring. After 4 h reaction under N_2 protection, the temperature was cooled to room temperature and CTS-modified magnetic nanoparticles (CTS-MNPs) were separated by an external magnet and washed several times with deionized water and ethanol alternately. Finally, CTS-MNPs were dried at 60 °C for 24 h under vacuum.

4. Preparation of PEI-Modified Magnetic Nanoparticles (PEI-MNPs)

Typically, 1 g CTS-MNPs and 1 g polyethylenimine (PEI) were dissolved in 100 mL deionized water and stirred at 50 °C for 5 h under N_2 protection. After cooling to room temperature, PEI-modified magnetic nanoparticles (PEI-MNPs) were separated by an external magnet, washed several times with deionized water and ethanol alternately, and dried at 60 °C for 24 h under vacuum.

5. Preparation of PEI-Modified Magnetic Hydrogel Nanocomposites (PEI-mHNAs)

Typically, the synthesis of PEI-modified magnetic hydrogel nanocomposite absorbents (PEI-mHNAs) is as follows: 10 g acrylic acid, 10 g acrylamide and 3.61 g NaOH are dissolved in 100 mL deionized water and stirred for 45 min at room temperature. Then, 3.0 g PEI-MNPs and 0.15 g polyethylene glycol diacrylate are added into the above monomer solution and stirred for 30 min at room temperature. After that, the temperature is raised to 60 °C, followed by the slow addition of 0.24 g ammonium persulfate and 0.077 g sodium bisulfite. The reaction mixture is stirred for 5 h at 60 °C. After cooling to room temperature, PEI-mHNAs are separated by an external magnet, washed several times with deionized water and ethanol alternately and left over night in ethanol. Finally, PEI-mHNAs are dried at 60 °C for 24 h under vacuum.

6. Heavy Metal Ions Adsorption Experiment Using Batch Methods

Batch adsorption experiments were carried out on a thermostatic shaker with a constant speed of 120 rpm at room temperature to study adsorption properties of heavy metal ions, such as Cu(II), Pb(II) and Cd(II) for PEI-mHNAs. 0.1 g dry and milled PEI-mHNAs was immersed in 100 mL heavy metal ions solution with desired initial concentration and pH for a given time at room temperature, and then heavy metal ions concentration left in the solution was analyzed by atomic absorption spectrometry.

Metal absorption capacity was calculated using the following equation:

$$q_e=(C_0-C_e)V/m \quad (1)$$

where q_e is the amount of metal ion adsorbed (mg/g), C_0 and C_e are initial and equilibrium concentration of metal ion (mg/L) in the testing solution, respectively. V is the volume of the metal ion solution (L) and m is the mass of dry PEI-mHNAs (g).

7. Recycling Experiments for PEI-mHNAs Towards Heavy Metal Ions

Absorbed heavy metal ions for PEI-mHNAs were desorbed with 0.5 M HCl solution for 90 min. After desorption, PEI-mHNAs were removed from desorption solution using an external magnet, and washed with distilled water, dried at 60 °C for 24 h, and used for the subsequent runs. To test the recycling performance of PEI-mHNAs, this adsorption-desorption cycle was repeated five times using the same adsorbents.

8. Characterization of the Magnetic Hydrogel Nanocomposite Absorbents

Morphologies of MNPs, CTS-MNPs and PEI-MNPs were observed by JEM-100CX transmission electron microscopy (TEM). The samples were dropped onto a copper net sprayed with carbon, dried in vacuum, and then tested on a transmission electron microscope with an acceleration voltage of 100 kV. The micrographs of PEI-mHNAs were observed by HITACHI S-530 scanning electron microscope (SEM). Before SEM observation, all samples were fixed on aluminum stubs and coated with gold. FTIR spectrum involved a Perkin-Elmer 1750 spectrophotometer, equipped with an Epson Endeavour II data station. The samples were prepared as

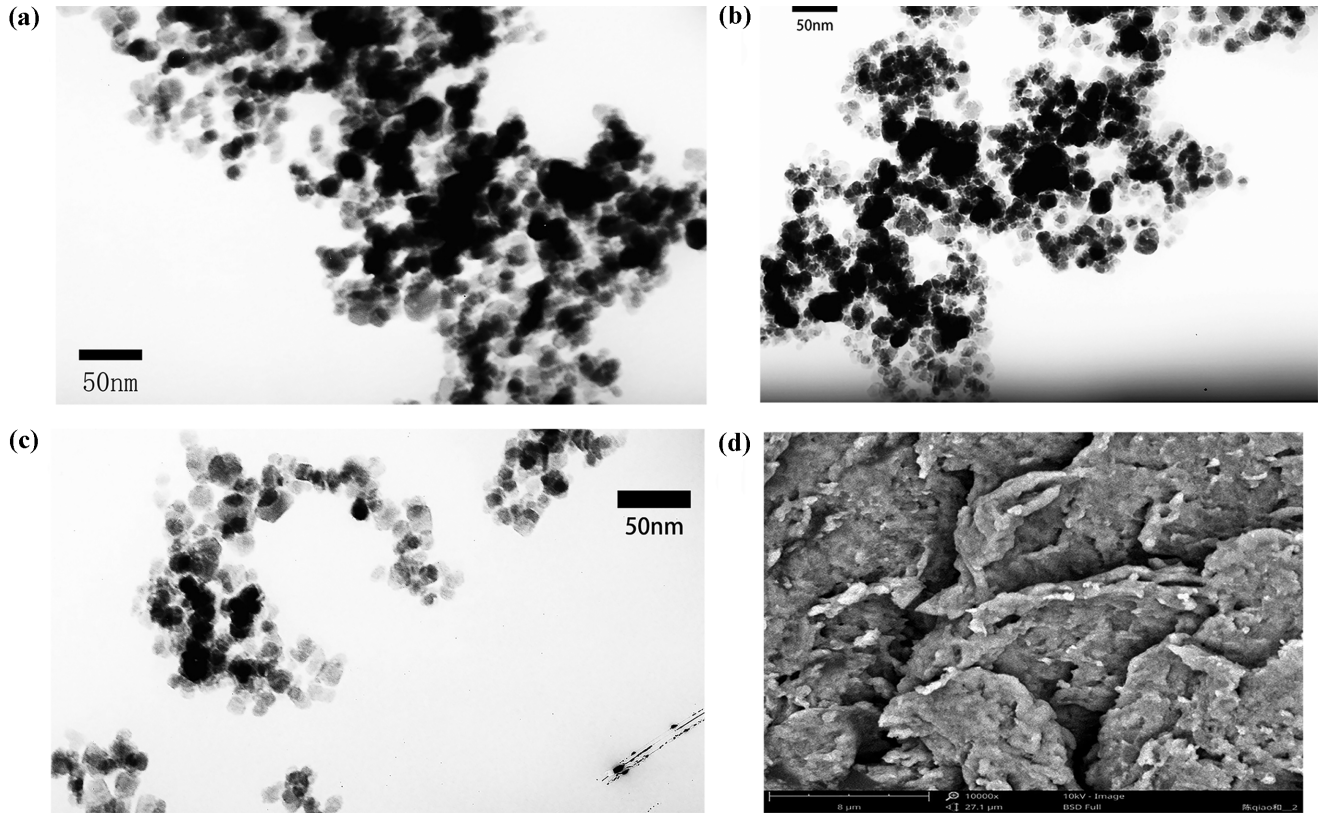

Fig. 1. TEM images of MNPs (a), CTS-MNPs (b) and PEI-MNPs (c). SEM image of PEI-mHNAs (d).

KBr pellets or as liquid films interposed between KBr discs. X-ray diffraction analysis was on a DMX-IIIC diffractometer. Magnetic properties were determined by a LakeShore 7407 vibrating sample magnetometer (VSM) at room temperature. Thermogravimetric analysis (TGA) was from room temperature to 600 °C with a heating rate of 10 °C/min under steady nitrogen.

RESULTS AND DISCUSSION

1. Feature of the Magnetic Materials

Fig. 1(a)-1(c) show the TEM images of MNPs, CTS-MNPs and PEI-MNPs, respectively. It can be seen from Fig. 1(a)-1(c) that MNPs, CTS-MNPs and PEI-MNPs have irregular particle shapes and partial agglomeration with average size of 15-20 nm. This may be related to the high-vacuum drying process of the TEM, during which the magnetic nanoparticles easily agglomerate. After surface modification with CTS and PEI, the agglomeration of magnetic nanoparticles is reduced due to the steric effect of the organic molecular chains grafted to the surface of magnetic nanoparticles [42].

As seen from Fig. 1(d), the surface of PEI-mHNAs is rough and uneven with many rough porous and interstitial structures. This structure can help heavy metal ions to rapidly penetrate and diffuse into the three-dimensional network of the magnetic polymer adsorbent, thereby enhancing the heavy metal adsorption of PEI-mHNAs.

2. FTIR and XRD Analysis of the Magnetic Materials

FTIR spectroscopy is used to identify the chemical groups present in magnetic materials. As seen from FTIR spectrum of MNPs (Fig. 2(a)), a broad and intense peak at around 3,439 cm is ascribed to O-H stretching vibration. Sharp and strong peak near 584 cm^{-1} is assigned to Fe-O functional groups [43]. Compared with absorption peaks of unmodified magnetic nanoparticles, some new absorption peaks appear for CTS-MNPs. Absorption peaks at 2,922 cm^{-1} and 1,131 cm^{-1} are attributed to the characteristic absorption peak of CH_2 and of Si-O bond [45], respectively, indicative of a successful graft of silane coupling agent onto the surface of magnetic Fe_3O_4 nanoparticles. As compared with absorption peaks of CTS-MNPs, some new absorption peaks occur for PEI-MNPs. 1,440 cm^{-1} is ascribed to the NH_2 bending vibration [44], and 3,865 cm^{-1} may be the N-H vibration absorption peak caused by the hydrogen bond of PEI molecular chain, indicating that PEI is successfully grafted onto the surface of silane coupling agent. After copolymerization of PEI-MNPs with functional monomers, the FTIR spectrum of PEI-mHNAs changes obviously. For example, 1,730 cm^{-1} is ascribed to carbonyl stretching vibration, 3,450 cm^{-1} is assigned to NH_2 and OH stretching vibration absorption, 1,458 cm^{-1} is attributed to the NH_2 and OH bending vibration [45], and 584 cm^{-1} is the characteristic absorption for magnetic Fe_3O_4 nanoparticles. The results show that PEI-mHNAs has been successfully prepared based on poly(acrylamide-co-acrylic acid) and PEI-MNPs.

As can be seen from XRD spectra (Fig. 3(b)), MNPs, CTS-MNPs and PEI-MNPs have sharp characteristic diffraction peaks at 2θ= 30.23°, 35.50°, 43.36°, 53.67°, 57.12° and 62.72°, corresponding to the (220), (311), (400), (422), (511) and (440) crystal faces of Fe_3O_4

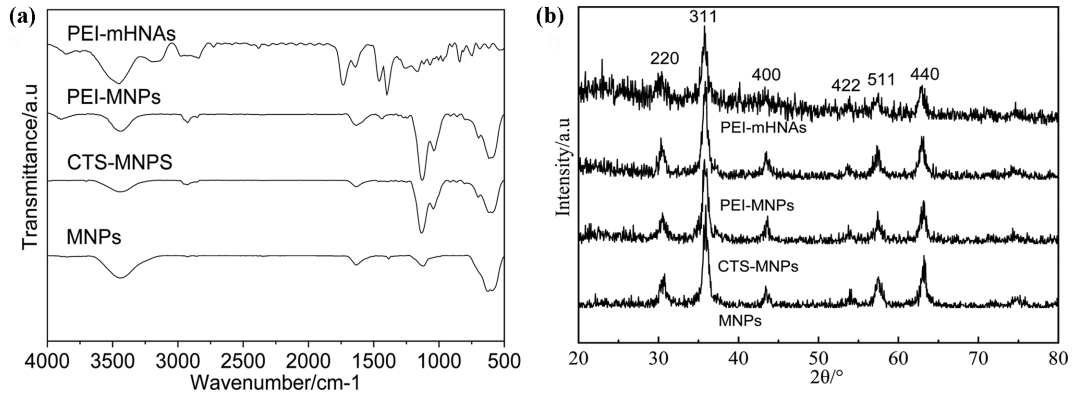

Fig. 2. FTIR (a) and XRD spectra(b) of MNPs, CTS-MNPs, PEI-MNPs and PEI-mHNAs.

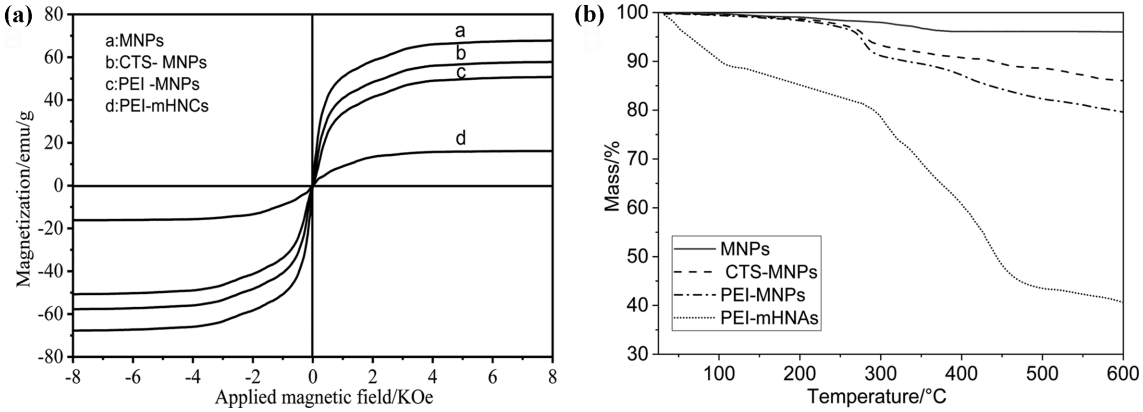

Fig. 3. Magnetization (a) and TGA curves (b) of MNPs, CTS-MNPs, PEI- MNPs and PEI-mHNAs.

cubic phase, respectively. These results are consistent with the characteristic diffraction peaks of standard Fe_3O_4 (JCPDS No. 19-06290). Note that PEI-mHNAs has characteristic diffraction peaks of standard magnetic Fe_3O_4 at 2θ=30.23°, 35.50°, 57.12° and 62.72°, indicating that the crystal structure of magnetic Fe_3O_4 is not destroyed during the radical copolymerization of acrylamide and acrylic acid.

3. Magnetic Property and TGA Analysis of Magnetic Materials

Magnetic hysteresis loop and TGA curves of magnetic materials are shown in Fig. 3. As shown in Fig. 3(a), saturation magnetization of MNPs reaches 67.76 emu/g. The saturation magnetization of Fe_3O_4 magnetic nanoparticles modified by CTS and PEI decreased slightly, and the saturation magnetization was 58.12 emu/g and 51.03 emu/g, respectively. Although the saturation magnetization of PEI-mHNAs is reduced to 16.47 emu/g due to the non-magnetic response of the silane coupling agent and the polymer matrix, PEI-mHNAs still has a certain magnetic response. In addition, we can also see that all magnetic materials are superparamagnetic due to their zero remanence and coercivity. Therefore, PEI-mHNAs can facilitate solid-liquid separation by an external magnet with the advantages of high separation efficiency, time, labor saving and no secondary pollution.

MNPs, CTS-MNPs and PEI-MNPs

TGA curve of MNPs (Fig. 3(b)) shows slight weight loss (3.8%) around 600 °C, which should be caused by the dehydration of hydroxyl groups on the surface of magnetic Fe_3O_4 nanoparticles during the heating process. This demonstrates that MNPs has high thermal stability. Weight loss of CTS-MNPs reached 13.7% from 270 °C to 600 °C due to the decomposition of the silane coupling agent grafted onto the surface of magnetic nanoparticles, indicating that silane coupling agent was successfully grafted onto the surface of magnetic nanoparticles with the content of about 13.7%. In comparison, residue for PEI-MNPs at 600 °C was 79.5%, from which we could calculate that the content of PEI chains was 6.8%, indicating that PEI chains were successfully grafted onto the surface of CTS-MNPs. Weight loss for PEI-mHNAs between 30-150 °C can be attributed to a small amount of evaporation of adsorbed water. Weight loss for PEI-mHNAs reached 37.5% between 280-500 °C, which was mainly ascribed to decomposition of polymeric matrix chains as well as silane coupling agent and PEI chains grafted onto magnetic nanoparticles. The thermal decomposition temperature of PEI-mHNAs exceeded 280 °C, indicating high thermal stability of PEI-mHNAs.

4. Effect of Acrylic Acid/Acrylamide Mass Ratio on Heavy Metal Ion Adsorption of PEI-mHNAs

Effect of acrylic acid/acrylamide mass ratio on heavy metal ion adsorption of PEI-mHNAs is presented in Fig. 4. Adsorption capacity of PEI-mHNAs for heavy metal ions Cu^{2+}, Cd^{2+} and Pb^{2+} increased first and then decreased with increasing acrylic acid/acrylamide mass ratio. When the mass ratio of acrylic acid/acrylamide was 60 : 40, the adsorption capacity of PEI-mHNAs for heavy metal

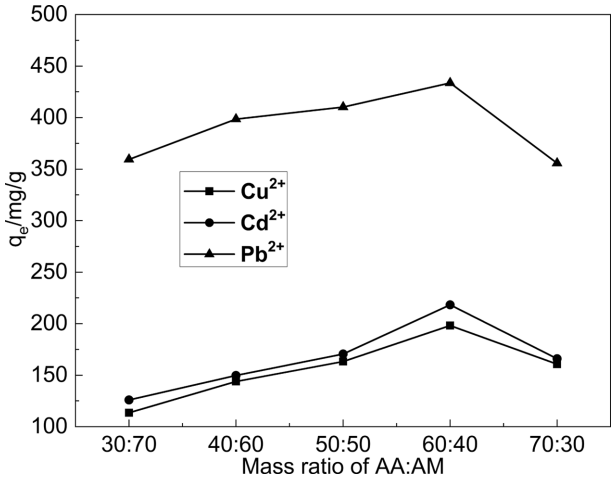

Fig. 4. Effects of AA/AM mass ratio on the adsorption capacity of copper, cadmium and lead ion for PEI-mHNAs.

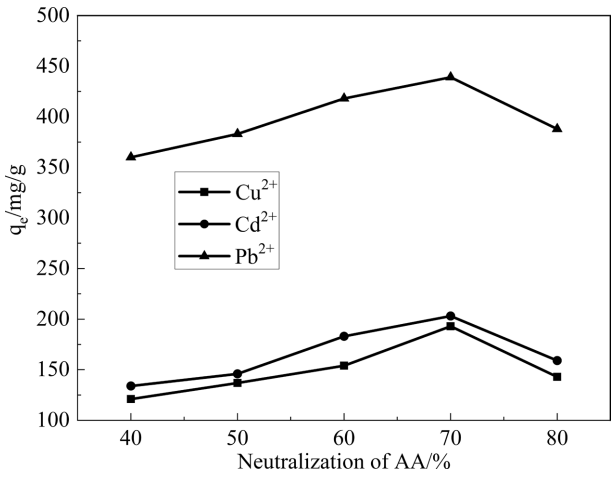

Fig. 5. Effects of neutralization degree of AA on the adsorption capacity of copper, cadmium and lead ion for PEI-mHNAs.

ions reached the maximum.

In general, both carboxyl group and amide group can adsorb heavy metal ions. COO^- can absorb heavy metal ions by way of chelating and electrostatic force with heavy metal ions, while $CONH_2$ absorbs heavy metal ions by complexation. Hence, COO^- group has higher heavy metal ion than $CONH_2$ group, and higher acrylic acid/acrylamide mass ratio can upgrade the heavy metals adsorption of the adsorbents. However, excessive acrylic acid/acrylamide mass ratio will reduce the heavy metals adsorption of the adsorbents. The greater the concentration of acrylic acid, the greater of the monomer reactivity, the faster of copolymerization, resulting in rapid temperature rise during radical copolymerization. This will lower the molecular weight of the polymer and form a dense polymer network structure, which is not conducive to the diffusion of heavy metal ions into the polymer gel network, and reduces the adsorption of heavy metal ions for PEI-mHNAs.

5. Effect of AA Neutralization Degree on Heavy Metal Ion Adsorption of PEI-mHNAs

Fig. 5 shows the effects of neutralization degree of AA on heavy metal ion adsorption capacity of PEI-mHNAs. Adsorption capacity of PEI-mHNAs for heavy metal ions Cu^{2+}, Cd^{2+} and Pb^{2+} increased with increasing AA neutralization degree. However, when AA neutralization degree was greater than 70%, the adsorption capacity of heavy metal ions of PEI modified magnetic polymer adsorbents decreased instead.

Copolymerization reactivity is relatively high at low AA neutralization degree due to the high reactivity of AA under acid condition, causing rapid copolymerization reaction rate, rapid temperature rise and dense polymer networks. Besides, the electrostatic repulsive force between polymer molecular chain is low under acidic conditions, which makes it difficult for heavy metal ions to diffuse and penetrate into the three-dimensional polymer network, thus reducing the adsorption of heavy metal ions for the absorbents. However, when AA neutralization degree is greater than 70%, the concentration of counterion Na^+ within the polymer network is high, resulting in an increasing shielding effect and reduction of the electrostatic repulsive force between the polymeric chains,

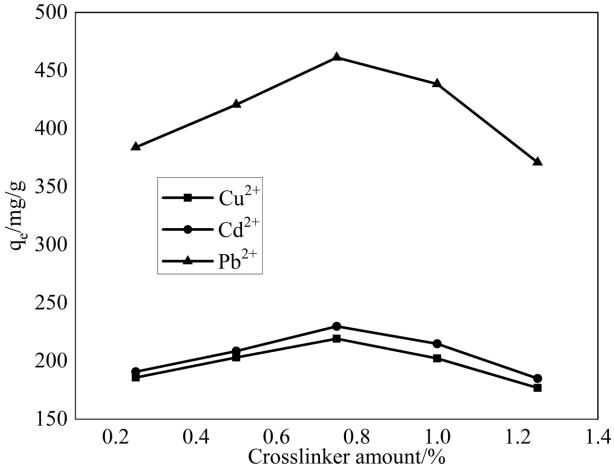

Fig. 6. Effects of crosslinker amount on the adsorption capacity of copper, cadmium and lead ion for PEI-mHNAs.

which is not beneficial to the expansion and extension of the polymer three-dimensional network, and reduces the adsorption capacity of heavy metal ions for PEI-mHNAs.

6. Effect of Crosslinker Amount on Heavy Metal Ion Adsorption of PEI-mHNAs

Crosslinker has a vital influence on the crosslinking density, mesh size, rigidity and strength of the polymer networks, and thus finally affects the heavy metals adsorption of the adsorbents. Fig. 6 shows the influence of crosslinker amount (based on AA and AM mass) on the heavy metal ion adsorption capacity of PEI-mHNAs. As can be seen from Fig. 6, when crosslinker amount was less than 0.75%, the adsorption capacity of heavy metal ions of PEI-mHNAs increased with the increase of crosslinker amount. However, when crosslinker amount was greater than 0.75%, the adsorption capacity of heavy metal ions of PEI-mHNAs decreased gradually. It is difficult to form a perfect three-dimensional polymer network when crosslinker amount is low, which is not conducive to the adsorption of heavy metal ions. However, excessive crosslinker will further increase the crosslinking density of the polymer network,

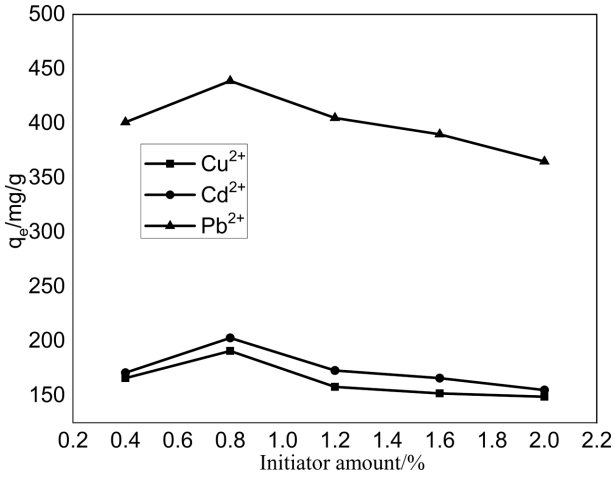

Fig. 7. Effects of initiator amount on the adsorption capacity of copper, cadmium and lead ion for PEI-mHNAs.

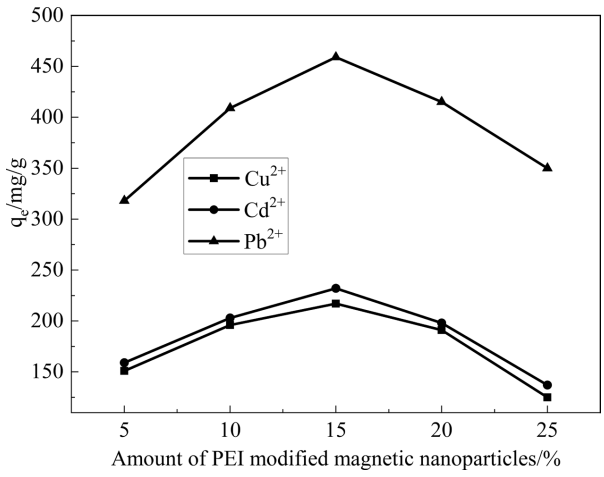

Fig. 8. Effects of PEI-MNPs amount on the adsorption capacity of copper, cadmium and lead ion for PEI-mHNAs.

forming more densely and rigidly polymer three-dimensional networks, making it difficult for heavy metal ions to penetrate into polymer networks. Therefore, too low or too high amount of cross-linker will both reduce the adsorption capacity of heavy metal ions for PEI-mHNAs.

7. Effect of Initiator Amount on Heavy Metal Ion Adsorption of PEI-mHNAs

Fig. 7 demonstrates the influence of initiator amount (based on AA and AM mass) on the heavy metal ions adsorption capacity of PEI-mHNAs. As can be seen, heavy metal ions adsorption capacity of PEI-mHNAs reached the maximum in the condition of 0.8% initiator. Too low or too high amount of initiator would reduce the adsorption capacity of heavy metal ions for PEI-mHNAs. When initiator amount is less than 0.8%, the reaction system has fewer free radicals, which leads to a low reaction rate and is not in favor of the formation of three-dimensional network structure. On the other hand, excess initiator can decompose and release a number of free radicals, which can reduce the molecular weight between polymeric network mesh, making the polymer network more dense and heavy metal ions more difficult to diffuse into the polymeric network. Hence, too low or too high amount of initiator will both reduce the adsorption capacity of heavy metal ions for PEI-mHNAs with the optimum amount of initiator of 0.8%.

8. Effect of PEI-MNPs Amount on Heavy Metal Ion Adsorption of PEI-mHNAs

Effects of PEI-MNPs amount (based on AA and AM mass) on heavy metal ion adsorption of PEI-mHNAs were studied and the results are shown in Fig. 8. Heavy metals absorption capacity increased when PEI-MNPs amount increased from 5% to 15%, and then decreased with further increasing amount of PEI-modified magnetic nanoparticles. When PEI-MNPs amount was 15%, PEI-mHNAs reached the maximal absorption capacity for Cu^{2+} (217 mg/g), Cd^{2+} (232 mg/g) and Pb^{2+} (459 mg/g).

With increasing amount of PEI-MNPs, more PEI macromolecules can interact via hydrogen bond and become entangled with polymer matrix molecules to form multi-level three-dimensional networks, which enhances the adsorption capacity of heavy metal ions for the adsorbent. In addition, PEI chains contain many amino and imine groups which have good adsorption for heavy metal ions. Consequently, the adsorption capacity of PEI-mHNAs for

Table 1. Adsorption capacities of heavy metals for various PEI adsorbents in the literature

Adsorbents	Maximum adsorption capacity (mg/g)	References
Alginate-PEI aerogel (Alg-PEI)	214.4 (Cu^{2+})	[45]
PEI functionalized magnetic Fe_3O_4	143 (Pb^{2+})	[46]
PEI-magnetic MNPs@SiO_2	143 (Cu^{2+})	[47]
DTPA grafted PEI-carboxylated GO	309.6 (Cu^{2+}), 316.2 (Pb^{2+})	[48]
Crosslinked PEI-dithiocarbamate	206 (Cd^{2+}), 215 (Cu^{2+}), 451.8 (Pb^{2+})	[49]
PEI-palm shell activated carbon	14.1 (Cd^{2+}), 53.5 (Pb^{2+})	[50]
PEI-bacterial cellulose	148 (Cu^{2+}), 141 (Pb^{2+})	[51]
Alginate/PEI hydrogel(Alg-PEI)	322.6 (Cu^{2+}), 344.8 (Pb^{2+})	[52]
PEI-immobilized pineapple fiber	273 (Cu^{2+}), 165 (Pb^{2+})	[53]
Nanocellulose/PEI aerogels	175.4 (Cu^{2+}), 357.4 (Pb^{2+})	[54]
Chitosan-graft-PEI-Dithiocarbamate	178.7 (Cd^{2+}), 138.9 (Cu^{2+}), 337.7 (Pb^{2+})	[55]
PEI-mHNAs	217 (Cu^{2+}), 232 (Cd^{2+}), 459 (Pb^{2+})	This work

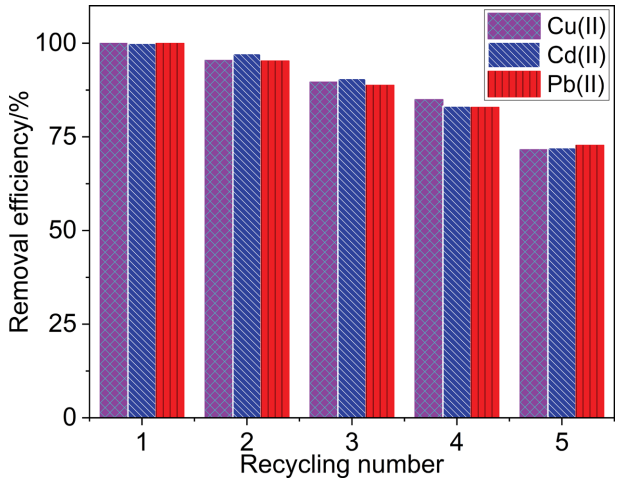

Fig. 9. Recycling performance for PEI-mHNAs toward heavy metal ions.

heavy metal ions increases with increasing PEI-MNPs amount. However, excessive PEI-MNPs have adverse effects on the heavy metal ions adsorption capacity of PEI-mHNAs. Acting as the physical crosslink point, excess PEI-MNPs will further increase the crosslinking density of the magnetic polymer adsorbents, making polymer chains difficult to stretch and expand, thus decreasing heavy metal ions adsorption capacity of PEI-mHNAs.

Comparing the heavy metals adsorption capacity of PEI-mHNAs with other PEI absorbents reported in the literature (Table 1), obviously, PEI-mHNAs has good heavy metals adsorption capacity and is better than most of the other PEI absorbents. This indicates that PEI-mHNAs is an excellent adsorbent, with huge potential in the practical application of the heavy metal ions removal.

9. Recycling of PEI-mHNAs for Heavy Metal Ions

The regeneration and reuse of adsorbents are important criteria for practical applications. Continuous adsorption-desorption experiments were conducted and the results are shown in Fig. 9. After five cycles, removal efficiency of heavy metal ions decreased to 71.6% (Cu(II)), 72.1% (Cd(II)) and 72.8% (Pb(II)) of those for the first absorption, indicating good reversibility of Cu(II), Cd(II) and Pb(II) and good recyclability for PEI-mHNAs. The decrease of removal efficiency may be caused by a few active sites not being released or incomplete desorption.

CONCLUSION

PEI-modified magnetic hydrogel nanocomposites (PEI-mHNAs) with three dimensional networks were prepared by radical copolymerization of acrylamide and acrylic acid in the presence of PEI-modified magnetic nanoparticles. FTIR and XRD results show that PEI-mHNAs were successfully prepared without destroying the high crystallinity of magnetic Fe_3O_4. PEI-mHNAs had high adsorption capacity of Cu(II) (217 mg/g), Cd(II) (232 mg/g) and Pb(II) (459 mg/g) because of its porous and interstitial structure and multiple adsorption groups. PEI-mHNAs had the maximal absorption capacity for heavy metal ions in the synthesis condition of acrylic acid/acrylamide mass ratio of 60 : 40, 0.8% initiator, AA neutralization degree of 70%, 0.75% crosslinker, and 15% PEI-modified magnetic nanoparticles. In addition, PEI-mHNAs had good magnetic responsiveness, thermal stability and recycling performance, making it a potential application in removing heavy metal ions from the aqueous solution.

ACKNOWLEDGEMENTS

This work was supported by the Key Research and Development Program of Sichuan province (Grant No. 2019YFG0264); Technology Foundation for Selected Overseas Chinese Scholar, Department of Personnel of Sichuan province (Grant No. 19BZ08-009); State Key Laboratory of Geohazard Prevention and Geoenvironment Protection (Grant No. SKLGP2018Z005).

REFERENCES

1. R. Sivashankar, A. B. Sathya, K. Vasantharaj and V. Sivasubramanian, *Environ. Nanotechnol. Monitor. Manage.*, **1-2**, 36 (2014).
2. B. L. Reza, R. Z. Hamid, E. B. Mohammad and N. Afshin, *J. Taiwan. Inst. Chem. E*, **45**(4), 1642 (2014).
3. Z. Dahaghin, H. Z. Mousavi and S. M. Sajjadi, *Food Chem.*, **237**, 275 (2017).
4. Y. He, Q. Liu, J. Hu, C. Zhao, C. Peng, Q. Yang, H. Wang and H. Liu, *Sep. Purif. Technol.*, **180**, 142 (2017).
5. J. Liu, C. Hu and Q. Huang, *Bioresour. Technol.*, **271**, 487 (2019).
6. W. Y. Jiang, Y. H. Xing, L. Y. Zhang, X. M. Guo, Y. W. Lu, M. Yang, J. Wang and G. T. Wei, *J. Appl. Polym. Sci.*, **138**, 49830 (2021).
7. H. Tang, W. J. Zhou, A. Lu and L. N. Zhang, *J. Mater. Sci.*, **49**, 123 (2014).
8. H. Gurer-Orhan, H. U. Sabir and H. Ozgunes, *Toxicology*, **195**, 147 (2004).
9. A. Moradi, P. N. Moghadam, R. Hasanzadeh and M. Sillanpaa, *RSC Adv.*, **7**, 433 (2017).
10. A. Mishra, A. Nath, P. P. Pande and R. Shankar, *J. Appl. Polym. Sci.*, **138**, 50242 (2021).
11. G. J. Joshiba, P. S. Kumar, F. C. Christopher, G. Pooja and V. V. Kumar, *Environ. Sci. Pollut., R*, **27**, 27202 (2020).
12. A. Saravannan, P. S. Kumar and A. A. Renita, *J. Clean. Prod.*, **172**, 92 (2018).
13. L. Semerjian, *Environ. Technol. Innov.*, **12**, 91 (2018).
14. M. Cegłowski, B. Gierczyk, M. Frankowski and L. Popenda, *React. Funct. Polym.*, **131**, 64 (2018).
15. R. R. V. Hemavathy, P. S. Kumar, S. Suganya, V. Swetha and S. J. Varjani, *Bioresour. Technol.*, **281**, 1 (2019).
16. A. Afkhami and R. Norooz-Asl, *Colloids. Surf. A. Physicochem. Eng. Asp.*, **346**, 52 (2009).
17. F. Chen, Q. Wu, Q. Lü, Y. Xu and Y. Yu, *Sep. Purif. Technol.*, **151**, 225 (2015).
18. F. H. M. Luzardo, F. G. Velasco, I. K. S. Correia, P. M. S. Silva and L. C. Salay, *Environ. Technol. Innov.*, **7**, 219 (2017).
19. N. Yin, K. Wang, X. Ya and Z. Li, D*esalination*, **430**, 120 (2018).
20. G. Neeraj, S. Krishnan, P. S. Kumar, K. V. Shriaishvarya and V. V. Kumar, *J. Mol. Liq.*, **214**, 335 (2015).
21. A. Z. M. Badruddozaa, Z. B. Z. Shawon, T. W. J. Danie, K. Hidajata and M. S. Uddin, *Carbohydr. Polym.*, **91**, 322 (2013).

22. L. Castro, L. M. Blazquez, F. Gonzalez, J. A. Munoz and A. Ballester, *Hydrometallurgy*, **179**, 44 (2018).
23. S. C. N. Tang and I. M. C. Lo, *Water. Res.*, **47**, 2613 (2013).
24. X. Liu, Q. Hu, Z. Fang, X. Zhang and B. Zhang, *Langmuir*, **25**, 3 (2009).
25. R. Xiong, Y. R. Wang, X. X. Zhang and C. H. Lu, *RSC Adv.*, **4**, 22632 (2014).
26. C. Shan, Z. Ma, M. Tong and J. Ni, *Water. Res.*, **69**, 252 (2015).
27. F. Ge, M. M. Li, H. Ye and B. X. Zhao, *J. Hazard. Mater.*, **211-212**, 366 (2012).
28. L. P. Jiang and P. Liu, *ACS Sustainable. Chem. Eng.*, **2**, 1785 (2014).
29. D. Horák, M. Trchová, M. J. Beneš, M. Veverka and E. Pollert, P*olymer*, **51**, 3116 (2010).
30. H. V. Tran, L. Dai Tran and T. N. Nguyen, *Mater. Sci. Eng. C*, **30**, 304 (2010).
31. G. Crini, *Prog. Polym. Sci.*, **30**, 38 (2005).
32. H. Wang, Y. J. Han, Y. Liu, T. Bai, H. Gao, P. Zhang, W. Wang and W. G. Liu, *J. Hazard. Mater.*, **213**, 258 (2012).
33. E. Ramirez, S. G. Burillo, C. Barrera-Diaz, G. Roa and B. Bilyeu, *J. Hazard. Mater.*, **192**, 432 (2011).
34. N. B. Milosavljevic, M. D. Ristic, A. A. Peric-Gruji, J. M. Fillipovic, S. B. Strbac, Z. L. Rakocevic and M. T. K. Krusic, *J. Hazard. Mater.*, **192**, 846 (2011).
35. X. Gong and T. Ngai, *Langmuir*, **29**, 5974 (2013).
36. S. W. Won, J. Park, J. Mao and Y. S. Yun, *Bioresour. Technol.*, **102**, 3888 (2011).
37. A. Wu, J. Jia and S. Luan, *Colloids. Surf. A*, **384**, 180 (2011).
38. B. Chen, X. S. Zhao, Y. Liu, B. G. Xu and X. J. Pan, *RSC Adv.*, **5**, 1398 (2015).
39. P. S. Kumar, C. Senthamarai and A. Durgadevi, *Environ. Prog. Sustain. Energy*, **33**, 28 (2014).
40. V. V. Kumar, S. Sivanesan and H. Cabana, *Sci. Total. Environ.*, **487**, 830 (2014).
41. K. S. Paripoorani, G. Ashwin, P. Vengatpriya, V. Ranjitha, S. Rupasree and V. V. Kumar, *J. Mol. Catal. B. Enzym.*, **113**, 47 (2015).
42. Y. Ding, F. Liu, Q. Jiang, B. Du and H. Sun, *J. Inorg. Organomet. Polym.*, **23**, 379 (2013).
43. S. Chandra and J. Bhattacharya, *J. Clean. Prod.*, **215**, 1123 (2019).
44. S. Shi, J. Yang, S. Liang, M. Li, Q. Gan, K. Xiao and J. Hu, *Sci. Total. Environ.*, **628-629**, 499 (2018).
45. M. Wang, Q. Yang, X. Q. Zhao and Z. Q. Wang, *Int. J. Biol. Macromol.*, **138**, 1079 (2019).
46. H. M. Jiang, M. L. Sun, J. Y. Xu, A. M. Lu and Y. Shi, *Clean-Soil, Air, Water*, **44**(9), 1146 (2016).
47. O. Plohl, M. Finšgar, S. Gyergyek, U. Ajdnik, I. Ban and L. F. Zemljič, *Nanomaterials*, **9**, 209 (2019).
48. J. F. Xi, L. Y. Zhang, W. T. Zheng, Q. L. Zeng, Y. He, Z. He and J. Y. Chen, *J. Mater. Sci.*, **56**, 18061 (2021).
49. S. Z. Hu, Y. Zhou, L. H. Zhou, Y. Huang and Q. L. Zeng, *Environ. Sci. Pollut. R.*, **27**, 2444 (2020)
50. C. Y. Yin, M. K. Aroua and W. M. A. W. Daud, *Water. Air. Soil. Pollut.*, **192**, 337 (2008).
51. X. C. Jin, Z. Y. Xiang, Q. G. Liu, Y. Chen and F. C. Lu, *Bioresour. Technol.*, **244**, 844 (2017).
52. C. B. Godiya, M. Liang, S. M. Sayeda, D. W. Li and X. L. Lu, *J. Environ. Manage.*, **232**, 829 (2019).
53. S. Tangtubtima and S. Saikrasun. *Bioresour. Technol. Rep.*, **7**, 100188 (2019).
54. J. Li, K. M. Zuo, W. B. Wu, Z. Y. Xu, Y. G. Yi, Y. Jing, H. Q. Dai and G. G. Fang, *Carbohyd. Polym.*, **196**, 376 (2018).
55. W. Zheng, R. R. Kuchukulla, X. N. Xu, D. D. Zhang, L. H. Zhou and Q. L. Zeng, *J. Polym. Environ.*, **30**, 653 (2022).